Mixing of Granular Materials in Slowly Rotated Containers

J. J. McCarthy, Troy Shinbrot, Guy Metcalfe, J. Eduardo Wolf, and Julio M. Ottino
Dept. of Chemical Engineering, Northwestern University, Evanston, IL 60208

Noncohesive granular materials in slowly rotated containers mix by discrete avalanches; such a process can be described mathematically as a mapping of avalanching wedges. A natural decomposition is thus proposed: a ***geometrical*** *part consisting of a mapping* ***wedge*** *→* ***wedge****, which captures large-scale aspects of the problem; a* ***dynamical*** *part confined to the avalanche itself, which captures details emanating from differences in size/density/morphology. Both viewpoints are developed and comparisons with experiments are used to verify the predictions of the models. In this article, we develop a model of granular mixing and show how to extend the model in order that it may: (1) handle complicated geometries, (2) be applicable for 3-D mixers, (3) rapidly test mixing enhancement strategies, and (4) incorporate differences in particle properties. In addition, an optimal fill level is determined for several 2-D mixing geometries, and a novel hybrid — geometrical/dynamical — computational technique is proposed. By merging the geometrical and dynamical viewpoints, this technique reduces the computational time of a typical molecular-dynamics-type simulation by a factor of 15. The ultimate goal is to provide fundamental understanding and tools for the rational design and optimization of granular mixing devices.*

Introduction

A fundamental understanding of mixing and blending of granular materials can be beneficial to a wide range of industries: pharmaceuticals, metallurgy, ceramics, composites, polymers, food processing, and agriculture, to name a few. Yet, in relation to its industrial prevalence, our understanding of granular mixing lags considerably when compared to that of, for example, liquid mixing (Ottino, 1990). While fundamental solids mixing mechanisms (Lacey, 1954) have been energetically studied by investigators over the years (see, for example, Weidenbaum, 1958; Hogg et al., 1966; Bridgewater et al., 1968, 1985), a synthesis of these fundamentals into a coherent mixing description has been elusive. In fact, despite a substantial amount of work done during the past few years in granular mechanics (Jaeger and Nagel, 1992; Behringer, 1993; Mehta, 1994; Weitz, 1994) and powder mixing (Bridgwater, 1976; Fan et al., 1990; Poux et al., 1991), we do not have a full understanding of even the simplest case of two identical powders in a slowly rotated container.

Correspondence concerning this article should be addressed to J. M. Ottino.
Current address of G. Metcalfe: CSIRO/DBCE Advanced Fluid Mechanics Laboratory, Box 56, Graham Rd., Highett, Victoria 3190, Australia.

Possibly the biggest hindrance to an understanding of slow solids mixing is that there is no accepted set of governing equations—as in the companion case of liquid mixing (Ottino, 1990). Moreover, due to the fact that stress in granular materials is principally carried in "stress chains" (Liu et al., 1995), it is not even assured that a continuum approach is generally applicable. This lack of a universal mathematical description can be attributed to the intrinsic physical complexity of these problems, and also, in part, to the difficulty in experimentally measuring the bulk properties—stress, strain, voidage, and so on—which would be necessary in a continuum description of a granular flow. While there have been notable advances in noninvasive experimental methods [positron tomography (Broadbelt et al., 1993); nuclear magnetic resonance (Nakagawa et al., 19943); and gamma ray tomography (Nikitidis et al., 1994)], which circumvent problems associated with bed opacity and allow for the measurement of valuable information—particle positions, velocity profiles, and void fraction—it is apparent that a continuum approach has achieved only limited success in mixing problems, the primary field of use being restricted to "fast flow" situations

(Campbell, 1989). Similarly, other approaches to modeling granular flows—statistical mechanics (Mehta and Edwards, 1989) and cellular automata (Baxter and Behringer, 1991)—while useful in certain regimes, are not general for all types of granular flow and have not been successfully used as a predictive tool in granular mixing.

In contrast, the interactions of individual grains pose a much more tractable problem, both experimentally and theoretically, and much is known in this area (Hertz, 1881; Mindlin, 1949). The ever increasing power and efficiency of modern computers, as well as the view that particle-particle interactions are relatively well understood, recently have prompted researchers to turn to molecular dynamics-like methods of investigation (Walton, 1993; Tsuji, 1993; Lee and Herrmann, 1993). This type of particle dynamics model seems tailor-made for mixing applications, where particle properties are allowed to vary on a particle-by-particle basis, and detailed mixed structure is easily captured and visualized. The application of these methods to mixing, however, is still in its infancy and much remains to be done.

In this article, we develop a model of granular mixing, verify it with experiments, and show how to extend the model in order that it may: (1) handle complicated geometries, (2) be applicable for 3-D mixers, (3) rapidly test mixing enhancement strategies, (4) incorporate different particle properties. Our philosophy throughout this article is to take the simplest description consistent with experiment and progressively expand its scope. A geometrical model for tumbler mixers is described, applied to a variety of simple 2-D geometries, and compared to experiment for mixing patterns, mixing rates, and mixing efficiencies. This method is used to test strategies for mixing enhancement in 2- and 3-D containers, stretching the ideas to include baffles, general nonconvex domains, and time-varying avalanches. This article also discusses physical effects not captured by geometric modeling alone and limitations of the purely geometric viewpoint. After a brief review of particle dynamics methods, we propose a novel way to combine particle dynamics with geometric modeling to create a highly efficient hybrid computational method. Finally, we conclude with an outlook on promising areas of inquiry in granular mixing.

Mixing by Tumbling: A Geometrical View

Tumblers are perhaps the most common of solids processing devices; industrial examples include mixers [such as horizontal drum mixers (Carley-Macauly and Donald, 1962); V-blenders (Carley-Macauly and Donald, 1964); and double-cone blenders (Wang and Fan, 1974)]; rotary furnaces such as coke calcining and alumina calcining kilns (Perron and Bui, 1990; Perron et al., 1992; Bui et al., 1993), as well as a variety of coating operations. A tumbler refers to any hollow vessel which is partially filled with granular material and rotated, so that a circulating flow is produced. Tumblers exhibit different flow regimes—avalanching, slumping, rolling, cascading, raining, and centrifuging—depending on the rotational speed (Zablotny, 1965), and the literature contains several naming conventions for these regimes. This article will focus primarily on the simplest regime—from the viewpoint of mixing and granular flow—the avalanching regime, where each avalanche completes its descent before another avalanche begins. The ideas, however, can be extended analytically with little difficulty to the case in which the avalanching wedges are infinitesimally small, thus presumably capturing some aspects of the case of the continuously avalanching regime (Peralt and Yorke, 1995). [The real case is more complicated; a continuously avalanching flow involves a lens-shaped moving layer with a shear-like velocity profile (Khakhar et al., 1997).]

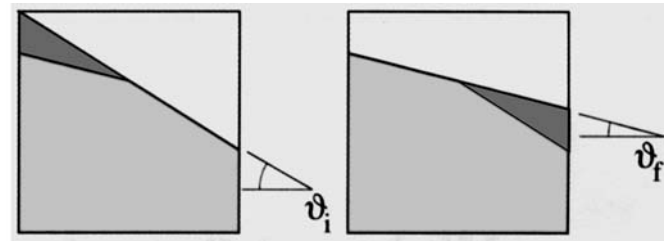

Figure 1. Movement of a wedge of material.

When a granular material exceeds its maximum angle of stability (left), an avalanche occurs and the surface relaxes to the material's angle of repose (right). When this avalanche occurs, the dark gray material moves from the top of the surface to the bottom as shown.

In a slowly rotated container, the bulk of the granular material moves as a solid body, while a wedge-shaped region periodically avalanches. When the granular material exceeds its maximum angle of stability, often termed its *dynamic* angle of repose, the elevated material falls down the free surface until the material reaches its *static* angle of repose. The net effect of this avalanche is that a quantity of material—a "wedge"—is moved from the upper portion of the surface to the lower portion of the surface (see Figure 1). Although the exact mechanism of the motion during an avalanche and the detailed dynamics involved are not well understood (this will be discussed more fully later), this simple geometrical fact yields valuable insights. The key observation is that the net transport in a slowly rotated container can be separated into two parts: transport of wedges (geometrical); and transport within wedges (dynamical). By decomposing the problem in this way, it is possible to study the implications of the geometry and dynamics separately and to add complexities in a controlled fashion. This allows even seemingly difficult problems (such as mixing in nonconvex geometries, and mixing of dissimilar particles) to be probed in a simple yet methodical way.

Simple Geometries

For problems involving the mixing of two similar, noncohesive powders—in the limit where they differ only in color—geometrical effects dominate and the mixing within a wedge is well described by one of the simplest wedge dynamics, perfect (random) mixing (Metcalfe et al., 1995). The most straightforward use of this approach is to study mixing in *uniformly-convex* 2-D containers such as a circle, a square, a triangle, and so on. In these geometries, the material is allowed to fall freely down the surface and the location of the avalanching material both before and after the avalanche is easily determined via conservation of mass (with the additional constraint that bed density remains constant, a simplifying assumption that does not cause perceptible error in the cases studied).

Figure 2 illustrates the behavior predicted by geometry alone. As a mixer slowly rotates, the material inside moves

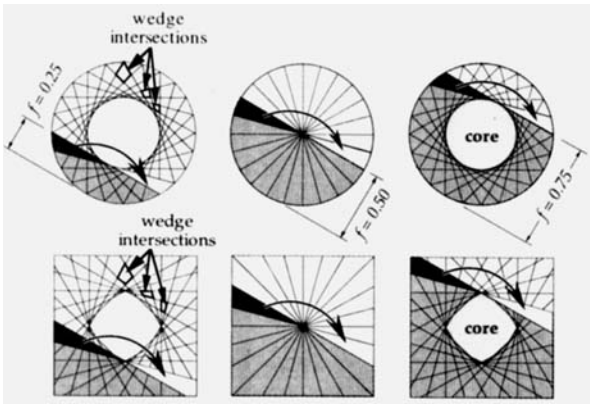

Figure 2. Motion of wedges in a circle and square shaped tumbling mixer.

Shown are three fill levels, $f = 0.25$, $f = 0.5$, $f = 0.75$. During an avalanche, the dark wedge falls to the position of the light wedge, and mixing occurs. Note the wedge intersections for $f = 0.25$ (that is, material in one wedge will enter a new wedge upon further rotation, enhancing interwedge mixing), there are no wedge intersections for $f = 0.5$, and the formation of a core for $f = 0.75$ (that is, centrally located material which never participates in an avalanche and therefore never mixes).

with the mixer as a solid body until it reaches the dynamic angle of repose. At this point, a wedge of material avalanches so that the material surface returns to a stable configuration. As previously mentioned, for two similar, noncohesive powders, a random map can be used to determine where the individual particles go within the destination wedge. This simple model captures the essential behavior of the system, which is characterized by f the fill level—the height to which the mixer has been filled with material. A comparison of mixing simulations with experiments in circular and triangular mixers is shown in Figure 3.

The key to understanding the mixing process lies in the quadrilateral intersections between wedges. For each fill level, one can draw a diagram to follow the motion of a wedge of material as it travels clockwise from its original position to its avalanche position (cf. Figure 2). Doing this demonstrates the relevance of the fill level. At low fill levels, there are many wedge intersections, so a portion of any wedge—a quadrilateral region—eventually finds itself being part of another wedge, thus enhancing interwedge mixing. As the fill level increases, a point is reached where the wedge intersections vanish. The mixing is slowed since no wedge of material can mix with any other wedge. In fact, this fill level, which occurs when the surface of the material remains above the center of mass of the mixer throughout the entire rotation, constitutes a minimum in the mixing rate (Wolf, 1995). Once past this fill level, another phenomenon occurs: core formation. Here, the wedges do not encompass the entire breadth of the material, and, as a result, a region of material—a core—does not get included in the avalanching process. This region only rotates with the mixer itself and does not get mixed at all. The core size increases with the fill level until finally the container is full, at which point no avalanching can occur and mixing stops.

From these observations of the model behavior, one can deduce that the efficiency of the mixer depends upon two important geometric entities: the fill level and the center of mass of the mixer. Obviously, material confined to the core does not participate in mixing, however, the material around the core mixes faster as the fill level increases and wedge intersections re-emerge.

The degree of mixing can be measured in terms of interfacial length per unit area (Mohanty et al., 1982). As mixing proceeds, the number of contacts between dissimilar particles increases; hence, the interfacial length per unit area (or in 3-D, the interfacial area per unit volume) increases. In the simulations, this length refers to the contact between particles on an imposed computational grid, while in the experiments this length is measured as contacts between pixels of a digitized image. The maximum value of the interfacial length per unit area for random mixing is one (Wolf, 1995).

For each fill level, the growth of the interface can be fit to an exponential curve. The product of the rate constant for the growth multiplied by the amount of material being mixed can be used as a measure of the overall mixing efficiency. Figure 4 shows computer simulation data of how the efficiency varies with fill level in the case of a circular mixer—these data are in agreement with experimental results (Metcalfe et al., 1995). For a circular cross-section, one can recognize core onset by the minimum, where mixing efficiency is nearly zero, which occurs at $f = 0.5$. It is interesting to note that the efficiency will only reach zero in the idealized case where the number of avalanches per revolution is an integer and the interface between the species lies on a wedge boundary. In real systems, neither condition will be met exactly and mixing will proceed slowly outward from the original wedge which contains the material interface. The data illustrate the presence of two maxima, one before and one after core onset. Clearly, the maximum which precedes core onset is more efficient and in general, except at fill levels very close to empty or to core onset, mixing is more efficient before core formation than afterwards. This trend holds true for all other geometries studied as well. A complete account, including asymmetric geometries, appears in Wolf (1995). Let us consider a few of the most important points.

The results for a computer simulation on an equilateral triangle appear in Figure 5. The efficiency of the maximum before core onset is almost ten percent higher than that for the circle at an approximately equal value of the mass fraction. Thus, for mixers of equal area filled to the same mass fraction, the triangle mixes more efficiently than the circle found in industry. A general survey of results for the shapes researched appears in Table 1.

3-D Geometries

As in the case of the 2-D geometries in the previous section, the first step towards building an understanding of the mixing process in 3-D rotated containers is to examine the idealized case of mechanically identical particles in a uniformly convex container. In 3-D rotated containers, wedge shapes vary in a complex way, but the same idea holds: avalanches move material from the upper portion of the surface to the lower, and mixing *within* the wedge of material occurs only during the avalanche. Similarly, the predictions made in the previous section (that is, faster mixing at low fill levels, formation of a core, and slower mixing at high fill levels) are still valid in describing the radial mixing, that is, mix-

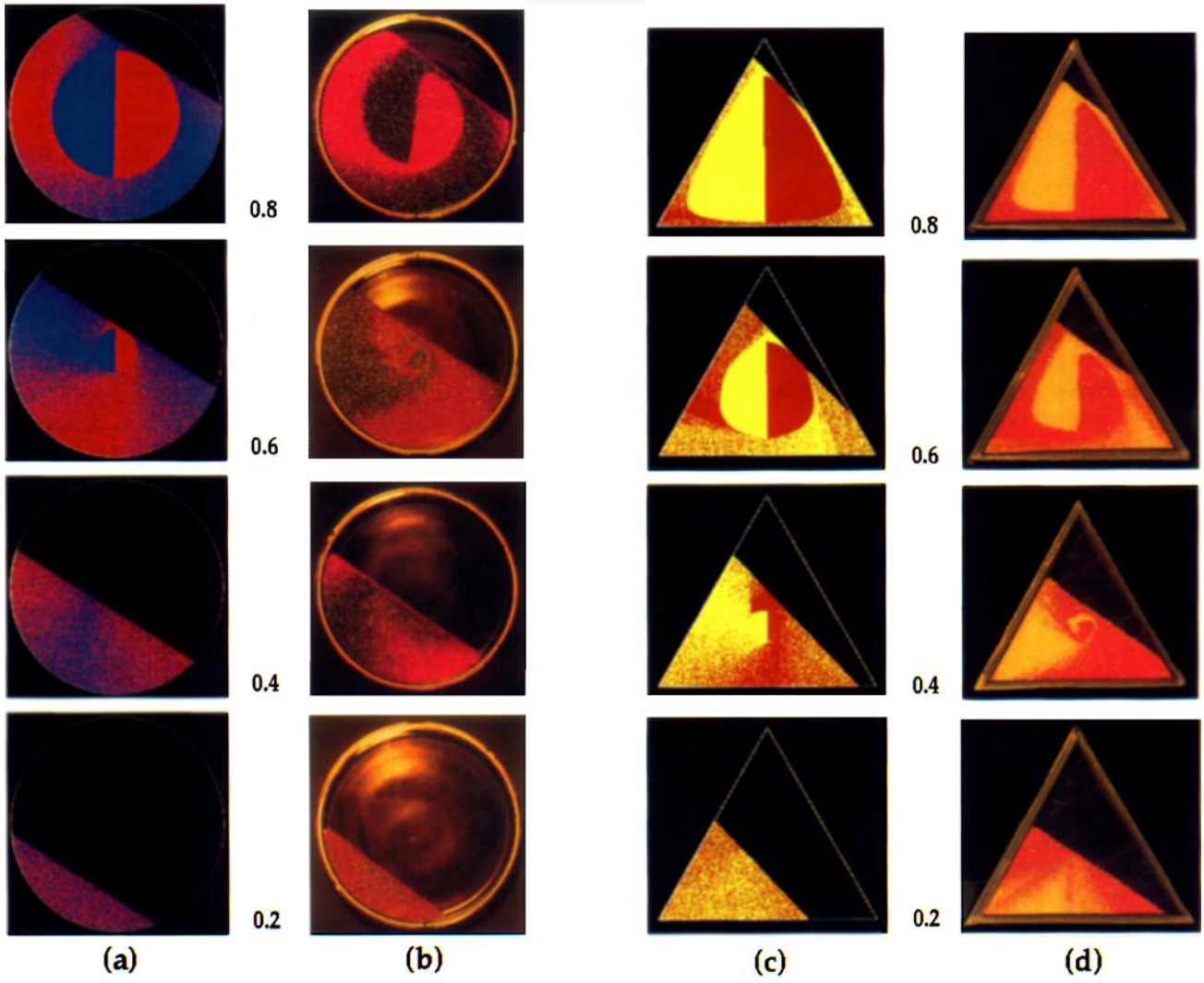

Figure 3. Mixing patterns from simulation and experiment after two revolutions at the indicated fill levels *f*.

Simulations (a,c) and experiments (b,d) for a circular and triangular cross section, respectively. To initialize an experiment (simulation), different colored material (red, blue; red, yellow) is loaded side by side with red on the right and blue (yellow) on the left.

ing perpendicular to the axis of rotation of the mixer. However, wedge movement alone provides no information regarding the axial mixing, that is, mixing parallel to the axis of rotation. In order to model the mixing within a 3-D wedge, some criterion for how the particles mix parallel to the axis of rotation must be incorporated into the dynamics within the wedge.

Several studies have dealt with axial mixing of mechanically identical particles (Hirosue, 1980; Rutgers, 1965; Carley-Macauly and Donald, 1962; Hogg et al., 1966a; Hwang and Hogg, 1980; Kaye and Sparrow, 1964). These investigations have demonstrated that this process is well described by a cross-sectionally averaged diffusion equation. Thus, for the case of mechanically identical particles, a 3-D map of the mixing within a wedge should have two parts, each described by random distributions. The radial mixing will occur via a uniform random distribution, while the axial mixing will occur via a Gaussian random distribution (Figure 6).

By making a straightforward modification of the random map of the previous section, diffusion parallel to the axis of rotation can be included and realistic simulation of 3-D wedges can be achieved. While the particles within the wedge still move randomly in the radial direction, the possible axial positions of the particles are weighted so that the probability of a particle moving a distance Δz along the mixer axis obeys a Gaussian distribution. This model can be verified as follows: consider a cylindrical mixer whose initial condition has a marker particle concentration of 1.0 for $-L < z < 0$ and 0.0 for $0 < z < L$. The centroid of the marker material begins at $z = 0.5 \cdot L$ and eventually decays to $z = 0$. By calculation of the centroid of either component, a quantitative comparison between theory, experiment, and simulation can be made. Figure 7 shows the position of the centroid of the marker particles vs. nondimensional time as calculated from a mixing simulation—using this model, the analytical solution of the diffusion equation and experimental data (Hogg et al., 1966b) —time is made dimensionless with the mixer length and the diffusion coefficient from the analytical solution.

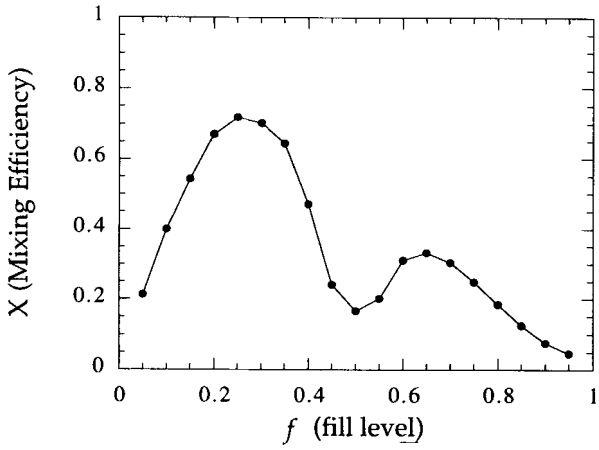

Figure 4. Mixing efficiency in a 2-D mixer with a circular cross-section.

For each fill level, the growth of the interface with time is fit to an exponential. The rate constant for the growth is multiplied by the amount of material being mixed, the core being excluded, to obtain the overall mixing efficiency. From this curve the optimum fill level is found to occur at approximately $f = 0.25$, and core onset occurs at $f = 0.5$.

Strategies for Mixing Enhancement

Using the geometric view of a tumbling mixer as expressed in the previous two sections, we can rapidly and easily explore strategies for mixer optimization. In this section we examine the role of baffles in the context of general nonconvex container shapes, and the effects on 3-D axial mixing of time-dependent changes to avalanching through the mechanism of wobbling.

Nonconvex/baffled geometries

Very little is known from a theoretical viewpoint about the effects of baffles on mixing of solids, even in cases restricted to 2-D situations. Our experiments indicate that baffles provide negligible function in most 2-D solids mixing applications, with a subtle exception. Judiciously deployed baffles can erode the unmixed core through a curious mechanism. Figure 8 shows a representation of the observed effect. An even number of uniformly spaced baffles have no effect on the core; similarly, baffles intruding into the mixing vessel do not affect the core behavior. However, an odd number of uniformly spaced, outwardly protruding baffles (or any number of nonuniformly spaced baffles) generate the following sequence of events. First, as shown in Figures 8a–8b, the protruding baffle partially fills with grains following an avalanche. However, a void (arrow) can be created when part of the baffle obstructs the flow. This void is typically sustained by arching of granular material above the baffle as the mixer continues to rotate (Figures 8b–8c). Finally, the arch collapses, and at that point the bulk of material in the container—including the core—shifts toward the baffle, as indicated in Figure 8d.

In controlled experiments in our laboratory, we have confirmed that although the cores of mixing containers with an odd number of uniformly spaced and protruding baffles steadily erode, no such effect is seen in vessels with simple intruding baffles, and their cores are static over time. Interestingly, vessels with uniformly spaced, even numbers of protruding baffles, do not erode their cores either. The reason for this is that in these vessels, each shifting event in one direction is paired with a shifting event in the opposite direction. So, although the core may be slightly smaller than it

Table 1. Efficiency Data for Various 2-D Shapes

Shape	Optimum Fill Level	Optimum Mass Fraction	Optimum Max. Efficiency	Core Onset Fill Level	Core Onset Mass Fraction	No. of Maxima
Circle	0.25	0.20	0.72	0.50	0.50	2
Hexagon	0.25	0.21	0.71	0.50	0.50	2
Pentagon	0.25	0.22	0.73	0.45	0.50	3
Square	0.25	0.25	0.73	0.50	0.50	2
Triangle	0.15	0.28	0.88	0.33	0.55	3

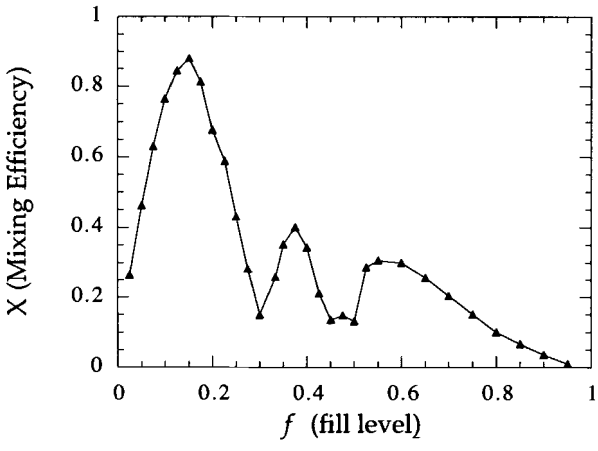

Figure 5. Mixing efficiency in a 2-D mixer with a triangular cross-section.

The overall mixing efficiency is calculated as in Figure 4. This geometry exhibits an overall optimum at approximately $f = 0.15$, a minimum at core onset ($f = 0.3$), and a second minimum at $f = 0.5$.

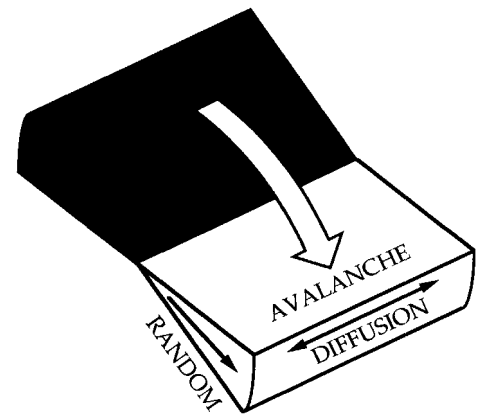

Figure 6. Mixing in a 3-D wedge of material.

For mechanically identical particles, when the upper wedge (gray) falls to the lower position (white), mixing along the axis of rotation is diffusive, and mixing in the radial direction is random.

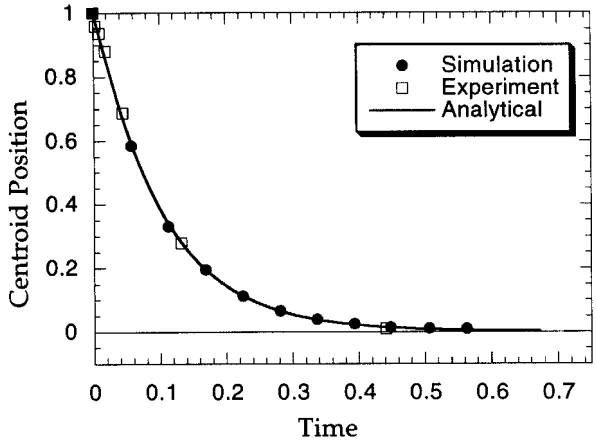

Figure 7. Axial mixing in a 3-D drum.

Axial mixing of granular materials can be modeled as a diffusive process. Shown is a comparison plot of the normalized position of the centroid of one of the species vs. dimensionless time for an experiment (Hogg et al., 1966b), a simulation using the 3-D model, and the analytical solution obtained using the diffusion equation.

would otherwise be, there is no steady motion of the core and it remains intact for essentially all time.

A final test of the mechanism illustrated in Figure 8 is depicted in Figure 9. If one constructs a chiral mixing container —such as the mixer in Figure 9—it is possible to obtain different mixing behaviors for different directions of rotation of the container. If we rotate the container shown in Figure 9 clockwise (top), the baffles should fill completely following an avalanche, while if we rotate it counterclockwise (bottom), a void can form within the baffles causing the core to shift as shown. Experiments confirm that this effect does occur as predicted (Figure 10).

Effects of wobbling

Tumbling mixers have been fashioned in a variety of shapes and configurations over the years in an attempt to produce more efficient mixing (Wang and Fan, 1974; Carley-Macauly and Donald, 1962, 1964). In most instances designs are *ad hoc*. However, with a full 3-D description of the geometrical effects in a tumbling mixer, new insights into the behavior of

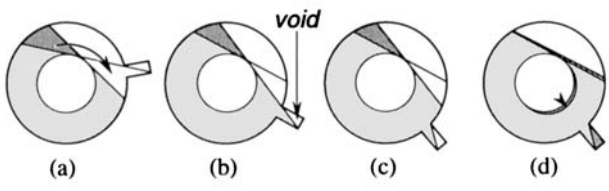

Figure 8. Core erosion.

Geometries with an odd number of uniformly spaced, outwardly protruding baffles erode the core. As the mixer rotates (a-d), an avalanche cannot completely fill the baffle and a void forms. Arching of the material will preserve this void for some time. When the arch collapses, the core shifts and a portion of the core enters the mixing region.

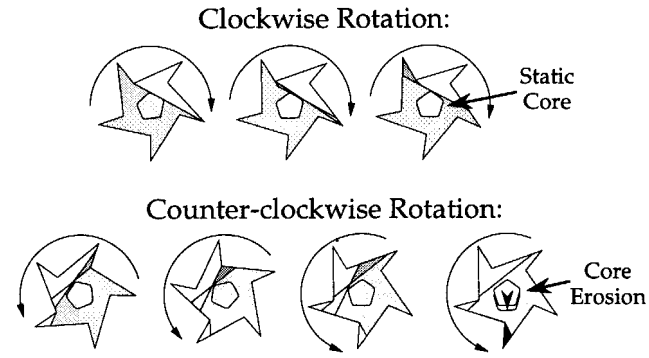

Figure 9. Core erosion in an asymmetric container.

Prediction: core erosion in chiral containers occurs for one direction of rotation but not another. Notice that for clockwise rotation, avalanches can freely fill arms of star, but not for counterclockwise rotation.

real slowly rotated mixers become available, and design improvements can be readily verified.

As was discussed in the previous section, axial transport in a tumbler limits the rate at which material can be mixed in a 3-D tumbler. There have been, over the past decade, ample demonstrations of the beneficial effects of time periodic operation in improving mixing efficiency in viscous fluids (Ottino et al., 1992). However, time periodic operation may leave unmixed islands which may be destroyed by other modes of operation (Franjione et al., 1989) or by combinations of two frequencies. Immediate parallels can be drawn with the present case of powder mixing (Wightman et al., 1995). Thus, one method of overcoming the obstacle of slow axial mixing is to wobble the tumbler—for example, for every revolution of the tumbler, allow the axis of rotation of the mixer to sinusoidally move vertically. Figure 11 shows this motion. In addition to avalanches perpendicular to the axis of rotation, which are caused by rotation alone, wobbling causes avalanches to

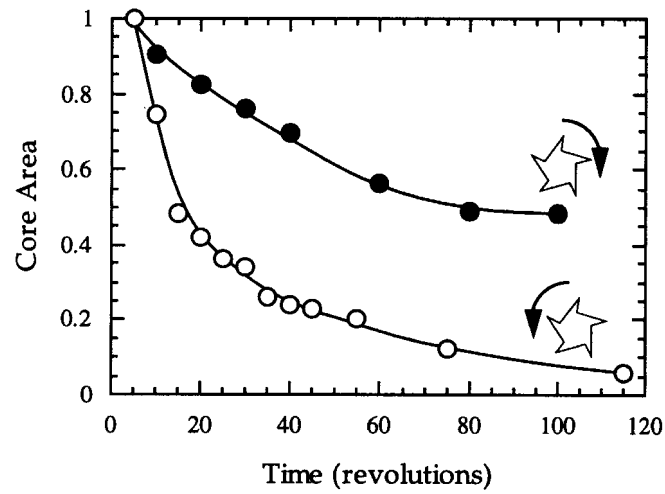

Figure 10. Core erosion in an asymmetric container.

Results of two core-erosion experiments with a bent star. In the first case the star was rotated counterclockwise and the core eroded by approximately 50%, in the second case the core eroded essentially completely.

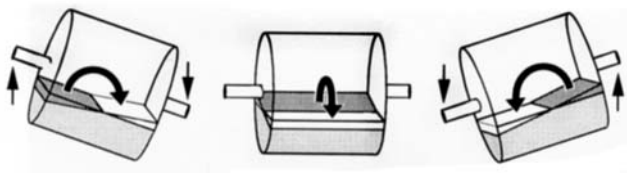

Figure 11. Wobbling motion.

Wobbling enhances axially mixing. When a drum is wobbled, avalanches occur along the mixer axis as well as perpendicular to the axis (as in a purely rotated drum).

occur parallel to the axis of rotation. These extra avalanches move material from one end of the tumbler to the other. Thus, the rapid radial mixing disperses the material more quickly than axial diffusion alone could, effectively enhancing axial transport.

Figure 12 shows the relative enhancement of axial transport as a function of the ratio of the number of avalanches—wobbling to rotational. The cylinder has an aspect ratio (length to diameter) of 2 to 1, and the mixer is filled to a fill level of $f = 0.4$. The wobbling motion is discrete—that is, in the one-to-one case, the cylinder is rotated until an avalanche occurs and then it is wobbled until an avalanche occurs and so on. It was found that this mixing protocol produces maximum mixedness at one wobbling avalanche per two rotational avalanches. This wobbling scheme is but one example of a mixer improvement whose effectiveness can be investigated quickly and easily with a 3-D model of a tumbling mixer.

Limitations of the Geometrical Viewpoint: Precession

The central core of Figure 3 can be a spectacular visual feature—and a spectacular impediment to mixing. In the model of the second section, the core has a purely geometrical origin, implying the core should appear for any material or container. Figure 13 illustrates this point. This case corresponds to the mixing of two powders with size, shape, and density differences—red particles are smaller, cubic, and more dense; green particles are larger, spherical, and less dense; the size ratio is about 3 to 1. While the core periphery is undoubtedly different than that in Figure 3, the geometrically predicted circular core is apparent.

Nevertheless, as we shall show, the core displays physical effects not contained in the simplest version of the model. In this section we show how the simplest geometric ideas about the core may be modified by inclusion of a surface boundary layer and a precessional rotation.

Further geometrical modeling can easily include the effect of the boundary layer. From geometrical considerations, we can calculate how the core grows with f. By assuming a boundary layer of width δ, we can calculate a reduction in size and a delay in onset due to the boundary layer. Then, by measurements of the core area vs. f we can back calculate δ. Interestingly, for the half dozen or so materials we have examined in this way, the boundary layer is consistently about 6 particle diameters. Agreement between the calculated δ and the visually observed boundary depth is a satisfying self-consistency check. Figure 14 compares two square-shaped mixers, a modified simulation including a boundary layer and an experiment. In this simulation, the boundary layer is included as follows: A typical boundary layer depth is chosen (here six particle diameters), the material down-slope of the avalanching wedge and within this depth is allowed to mix within itself, but not with the newly formed wedge, as it is sheared by the passing avalanche. One mechanism, core precession, however, cannot be captured by geometry alone.

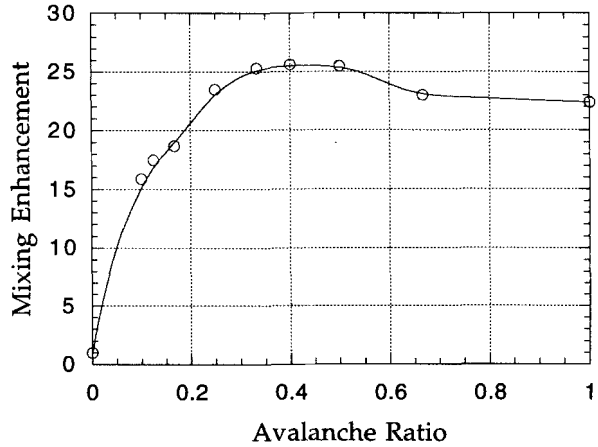

Figure 12. Axial mixing enhancement as a function of the ratio of the number of avalanches.

Ratio of the effective diffusion coefficient for a wobbling simulation to that of pure diffusion (no wobbling), are plotted vs. the ratio of the number of avalanches—wobbling to rotational. Note that a maximum occurs at one wobbling avalanche per two rotational avalanches.

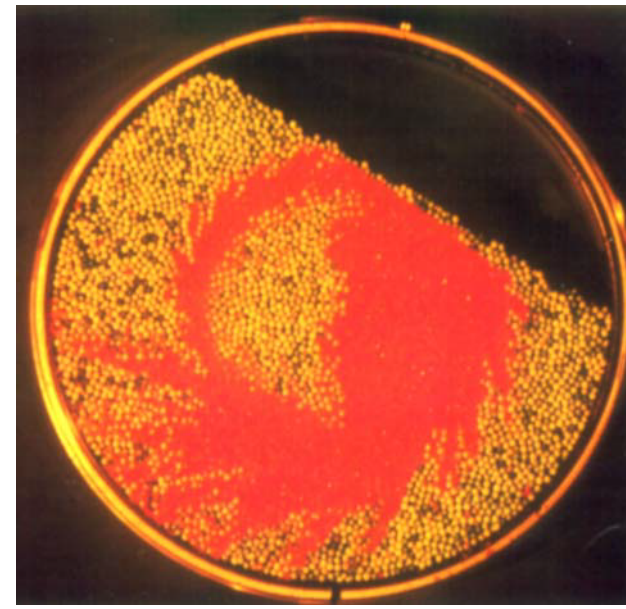

Figure 13. Geometrical origin of the core.

The materials being mixed are small, dense, cubic particles and large, light, spherical particles. Mixing within wedges is dramatically different than in Figure 3; however, the core is evident despite this difference.

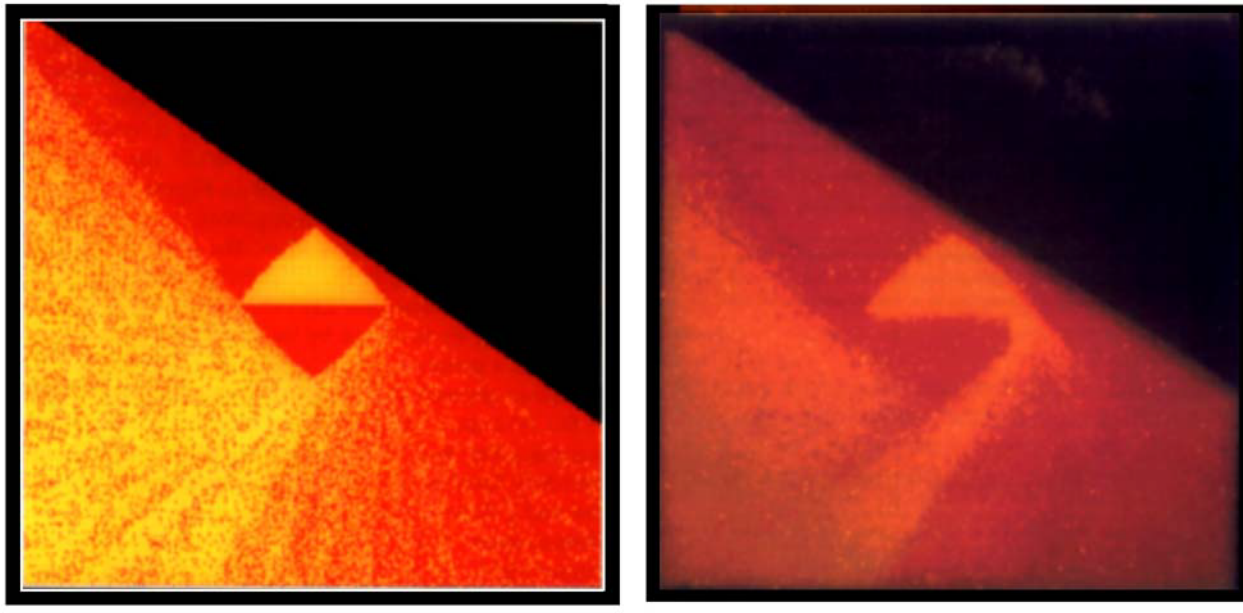

Figure 14. Mixing simulation including a boundary layer.

A comparison of an experiment and a simulation of a 2-D mixer with a square cross-section. Here, the simulation is modified in order to include a thin surface boundary layer.

Core precession is illustrated in Figure 15. After every full revolution of the container, the line demarking the initial interface between the colored grains should return to its original orientation. For a small number of revolutions, it does appear to do so. However, for a large number of revolutions —the exact number of revolutions differs for each material, yet it is generally well beyond a practical number of revolutions for mixing—the phenomenon is clearly evident (cf. Figure 15). The line rotates past its original position in the direction of the container rotation. While precession does not affect mixing in a circular mixer, it is nevertheless relevant to mixing in noncircular containers whose cores are not rota-

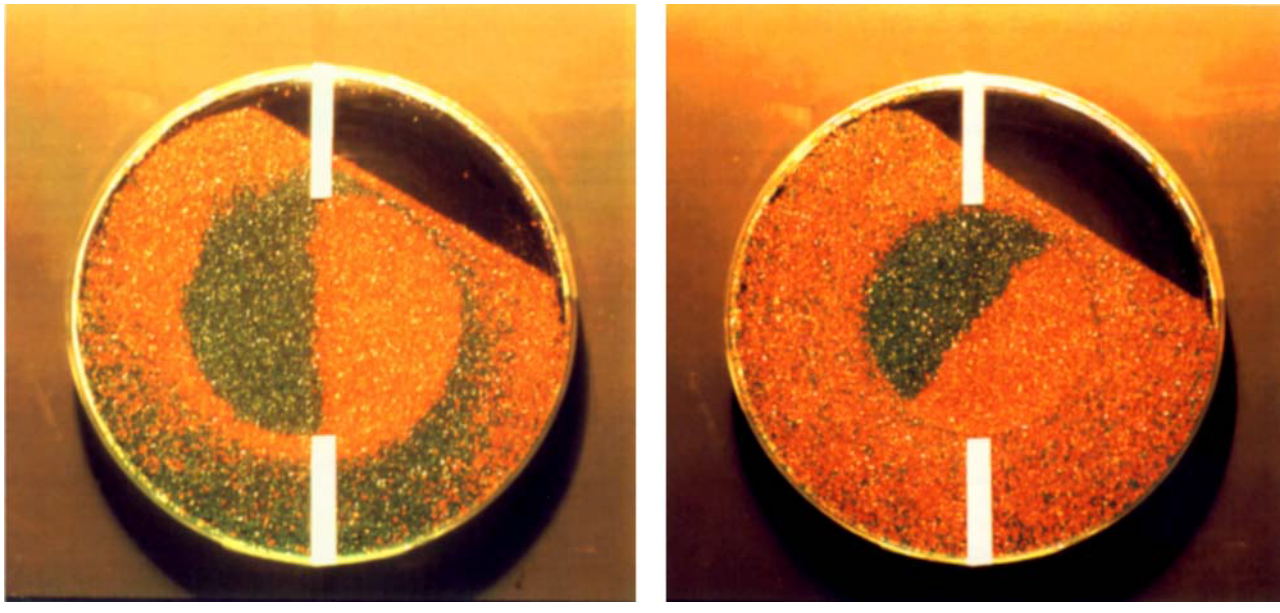

Figure 15. Core precession.

A comparison between two experimental photos of a 2-D mixer with a circular cross-section filled with large cubic particles. The first photo (a) is after 3 revolutions and the second (b) is after 40 revolutions. Note that the interface within the core has precessed by 42 degrees.

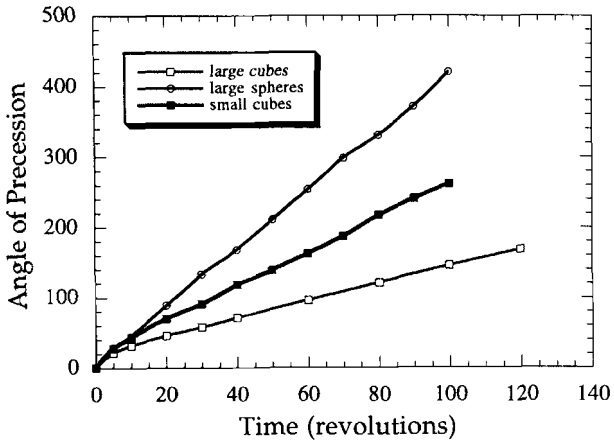

Figure 16. Precession rates by material.

Different materials precess at different rates. Shown is a comparison of the precession rates of large spherical particles, large cubic particles, and small cubic particles. The slope of the lines yield precession rates. Note that there is more than an order of magnitude difference between the precession rate of the large spherical particles and the large cubic particles.

tionally symmetric. Precession rotates these cores into the mixing zones where the corners are sheared off, ultimately decreasing the size of the core.

Preliminary experiments have led to three observations regarding core precession. (1) Precession depends on the container shape. Precession is observed in containers of about equal width to height ratios—the core does not seem to precess in long, thin containers. (2) The precession rate, that is, how many degrees θ_p the core precesses per container revolution, depends on the fill level f—the rate is highest just above half full and falls to zero for a completely full container. (3) The precession rate depends on the material being mixed.

Figure 16 shows precession measurements for several materials. Precession is linear. (At least at the sampling rate used. We cannot rule out the possibility that finer measurements would reveal θ_p moving in small jumps.) Therefore, the precession rates can be obtained from the slopes of the lines in Figure 16. There is an order of magnitude difference in the rate of change of the angle, $\dot{\theta}_p$, between small, cubic salt cubes and larger, spherical sugar balls. Since the precession rate depends on the material, core precession is an effect that does not seem explainable from geometry alone.

The physical mechanism driving core precession is at present obscure, but capturing the behavior may offer a validating test for future dynamical models of granular mixing, including the particle dynamics models we describe next.

Particle Dynamics

We have shown that—for slowly rotated mixers—geometrical and dynamical aspects of mixing can be decoupled. Investigating purely the geometrical aspects can yield considerable insight and implications of industrial importance, yet even slight differences in particle properties may change the dynamical aspects drastically. While the geometrical observations remain valid, an accurate analysis of the transport within the wedges becomes vital to a full understanding of the mixing. When materials with *different* properties are used, random mixing no longer suffices and the complex dynamics of mixing—and segregation—within a wedge must be more realistically incorporated. As it stands, the model in the previous sections cannot answer the following question: how well or poorly will a given combination of materials mix? Moreover, as briefly illustrated in the case of nonconvex geometries discussed earlier, in complex geometries it is not obvious where avalanching material will come to rest. By combining particle dynamics techniques with the geometrical model outlined in the previous sections, these difficulties can be alleviated.

Particle dynamics simulations capture the macroscopic flow of granular materials by calculation of individual particle trajectories. The time evolution of these trajectories then determines the flow of the granular material. Depending on the density and character of the flow to be modeled, different methods of calculating the trajectories are employed: a rigid particle model for low density, fast flow (the *grain-inertia* regime; Campbell and Brennen, 1985); or a soft particle model for high density, slow flow (the *quasi-static* regime; Walton, 1984).

In the *quasi-static* regime, encountered in a slowly rotated container, lasting contacts are important and particle density is high; thus, a soft particle approach is used (Cundall and Strack, 1979). In this model, particle trajectories are determined by solving Newton's equations of motion for each particle, where the forces on particles are described by a contact-dependent force law. The collisions/contacts in this model occur simultaneously and have finite duration. The particles are allowed to deform, or computationally overlap, and the restoring force of the deformed particle is generally chosen to agree with Hertz's (1881) contact theory, with a damping term to provide inelasticity. Similarly, the force on a particle subject to a tangential load is modeled after the work by Mindlin (1949). These force models have been essentially unchanged since Cundall and Strack's (1979) pioneering work. A notable exception is the model employed by Walton and Braun (1993). In their work, a partially latched spring is used in the normal direction, and an incrementally slipping friction model, fashioned after the work of Mindlin (1949), is used in the tangential direction.

Numerous investigators have utilized a soft particle method in modeling a variety of applications, such as chute flow (Walton, 1993), heap formation (Buchholtz and Poschel, 1994; Lee and Herrmann, 1993), avalanching (Lee, 1993), hopper flow (Tsuji, 1993), and rotating containers (Walton and Braun, 1993; Tsuji, 1993). While more computationally intensive than the rigid particle model, the soft particle method is quite versatile, capturing both rapid and quasi-static flows with accuracy (Tsuji et al., 1992).

In what follows we employ force laws similar to those of Cundall and Strack (1979). Forces in the normal and tangential directions are modeled as nonlinear and linear springs, respectively. Hertz (1881) found that the restoring force of two deformed elastic spheres in contact is given by

$$f_{n,e} = k_n \alpha^{3/2}$$

where α is the difference between the particle separation and the sum of their radii (m), and k_n is the normal spring

constant ($kg/\sqrt{m}\cdot s^2$)—which is related to the Young's modulus Y (N/m^2) and the Poisson ratio σ by

$$k_n = \frac{\sqrt{2a}\,Y}{3(1-\sigma^2)}$$

where a is the radius of the particle. Similarly, a simplified version of Mindlin's (1949) relation between tangential force and displacement is given by

$$f_t = -k_t s$$

where s is the relative tangential displace of the particles (m) since they first came in contact with each other and k_t is the tangential spring constant (kg/s^2)—which is related to the normal spring constant by

$$k_t = K \cdot k_n \sqrt{\alpha}$$

where K is a proportionality constant which depends on the Poisson ratio. Dissipation terms are then added to these forces to provide realistic particle responses. A dashpot (viscous dissipation term) in the normal direction provides collision inelasticity—the form is chosen such that normal collisions agree with experimental observations, while tangential dissipation is provided by limiting the tangential force to the Coulomb friction law. The complete force laws for the normal, f_n, and tangential, f_t, directions then become

$$f_n = k_n \alpha^{3/2} - k_d \upsilon_n \alpha$$

$$f_t = -\min(k_t s, \mu f_n)$$

The negative sign in the tangential force expression denotes the direction opposite of s. A schematic representation of these force laws is shown in Figure 17. These forces depend on particle collisions/contacts and are integrated for each particle to determine the particle's trajectory. The collision/contact search is performed using an indexed nearest-neighbor algorithm, such that the computational time increases with the number of particles N approximately as $N \cdot \log(N)$.

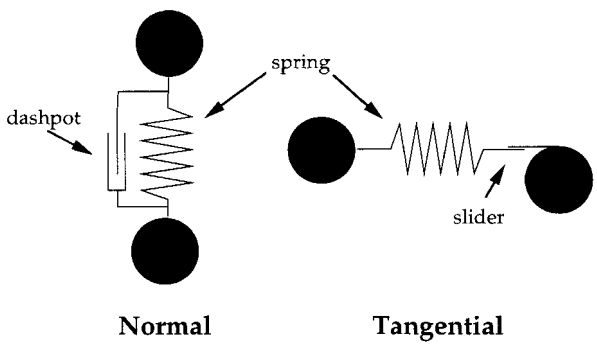

Figure 17. Particle dynamic force model.

Typical normal and tangential forces in a soft particle model, composed of a spring, dashpot and slider.

Merging Geometrical and Dynamical Approaches

Despite current capabilities and even the prospects of faster machines in the near future, it is however apparent that some problems of industrial importance may still be out of reach. Current particle dynamics simulations in the literature generally handle approximately 3,000–5,000 particles, whereas a typical industrial mixer may easily contain as many as 10^9 particles—six orders of magnitude more. Clearly, there are limits to the problem sizes than can be handled by particle dynamics models, but it may be possible to model industrial mixers despite these daunting numbers. By combining particle dynamics techniques with a geometrically based overview, it is possible to limit the number of particles necessary in a given simulation.

In a slowly rotated container, where particle motion consists of discrete avalanches, nontrivial dynamics are principally confined to the avalanching wedge, and the large-scale aspects of the problem can be easily handled by a geometrical approach. Confining the dynamics only where it matters —the avalanching wedge of material—results in substantial savings of computing time with respect to a full particle dynamics simulation.

This hybrid simulation technique utilizes the geometrical model of the second section with the particle dynamics techniques of the eighth section. First, the gross motion of the particles—solid body rotation—and identification of the particles within the avalanching wedge are accomplished using the geometrical model alone. At that point, a particle dynamics simulation, which includes the particles within the wedge as well as a boundary layer of particles—chosen such that increasing the size of the boundary layer caused no change in the result—is used to determine the small-scale dynamics of the avalanche itself. Once the avalanche is completed, the wedge particles are reassimilated into the bulk, and the geometrical model is used once again. By including only those particles predetermined by geometry to be within the wedge (including a shear boundary layer of approximately 5–10 particles), the number of particles involved in a particle dynamics simulation is typically 1/15 that of the full mixer simulation—this number depends on the fill level f.

This increase in computational speed allows simulation of as many as 75,000 particles to be accomplished in a reasonable period of time, while maintaining the versatility of a particle dynamics simulation. In addition, different particle properties, such as size/shape/morphology, are easily incorporated. Figure 18 shows a comparison of the mixing in an experiment and simulation. The experiment consists of small, cubic, dense particles and larger, spherical, less dense particles; the simulation, on the other hand, involves small, dense particles and large, less dense particles, both being spherical. Due to the fact that the parameters necessary to match the simulation to the experiment are not known—that is, Young's modulus, Poisson ratio, coefficient of restitution, angle of internal friction, and so on—no attempt was made to achieve a precise match. Instead, a comparison is made here in order to show that it is indeed possible to model segregation effects similar to those found experimentally by using this method. It is apparent that in both the simulation and the experiment the combination of materials does not mix well—radial segregation of the particles is clearly evident. This simulation technique easily captures the large-scale, geometrical fea-

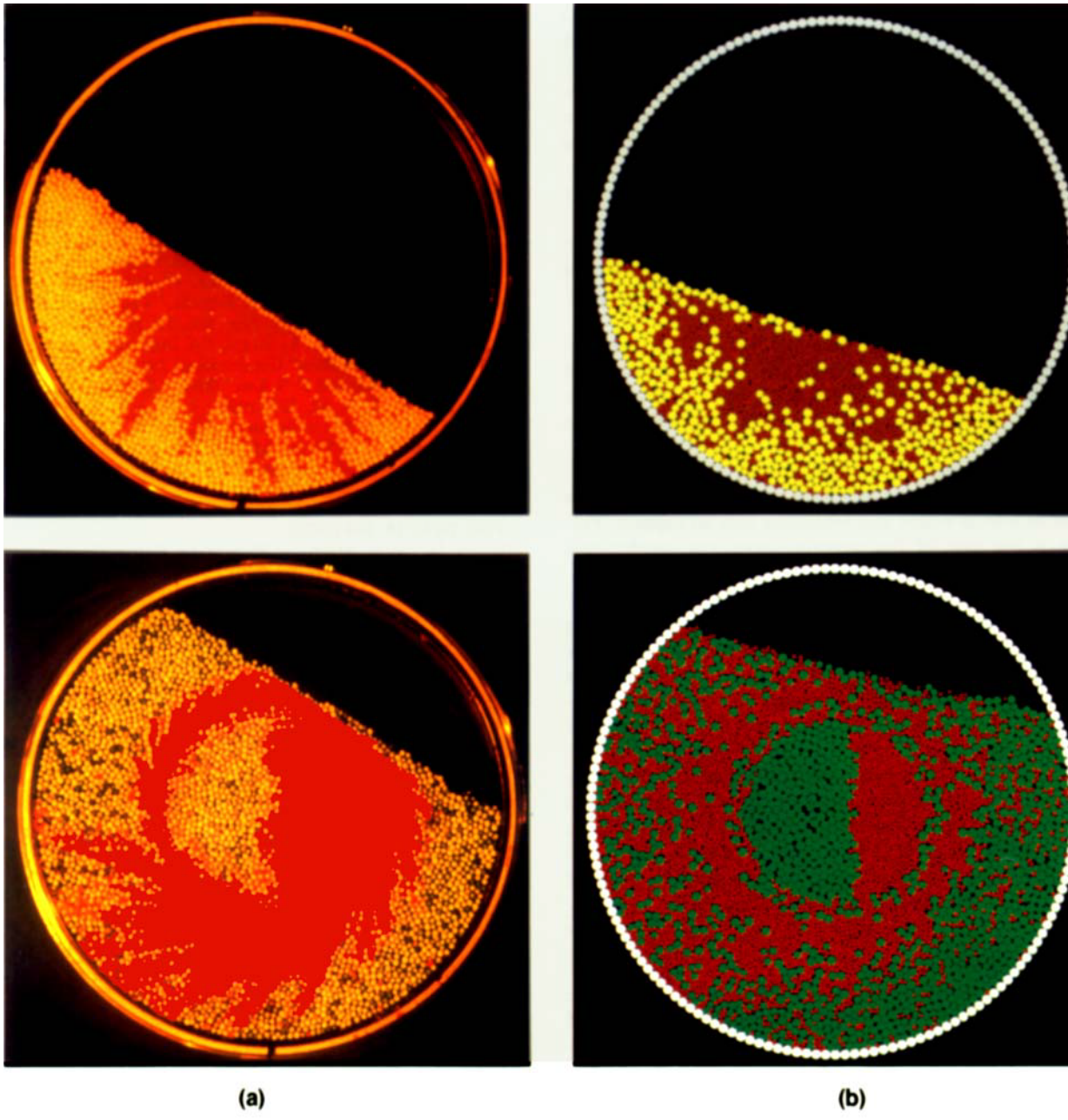

Figure 18. Experiment vs. simulation using the hybrid method.

Shown is a comparison of experiments (a) and simulations (b) of segregating materials at $f = 0.4$ and $f = 0.75$. The simulations easily capture the large-scale, geometrical features, such as the core, as well as the smaller-scale, dynamical characteristics like radial segregation. The simulation at the top involves 3,000 particles; the simulation at the bottom, 6,000 particles.

tures, such as the core, as well as the smaller-scale, dynamical characteristics like radial segregation.

Outlook

In this article we developed a picture of mixing of granular materials in simple tumblers that can be extended to more complicated, and industrially relevant, problems. In its simplest form—mixing of two identical cohesionless powders—the model can be used to predict mixing rates and efficiencies in a variety of 2-D mixer geometries. The agreement that we have found between the experiment and the model has been equally good at all fill levels, and results are generated in a tiny fraction of the computational time required by particle-dynamics methods.

Two-dimensional systems, when filled enough, lead to the formation of unmixed cores. It was found that a mixer with a triangular cross-section—whose optimum occurs at $f = 0.15$—is more efficient than the typical circular cross-section mixer—whose optimum occurs at $f = 0.25$. This technique is

easily extendible to include 3-D containers. By including diffusion along the mixer axis, realistic simulation of simple 3-D containers can be achieved. Agreement with experimental data is found in this case as well.

This model can also be used to examine and screen methods of mixer optimization. Some of the findings are new: even numbers of uniformly spaced, outwardly protruding baffles or any number of inwardly protruding baffles do not affect mixing in 2-D systems; however, nonuniformly spaced, outwardly protruding baffles or odd numbers of uniformly spaced, outwardly protruding baffles can be used to erode the unmixed core. Even more unexpected is the finding that some chiral geometries—such as "bent stars"—may mix very differently according to the sense of rotation.

It has been demonstrated as well that axial mixing in a drum mixer can be greatly enhanced by altering the protocol of motion of the drum. By wobbling the drum—sinusoidally moving the drum axis vertically—axial mixing rates can be increased by as much as a factor of 25.

While the geometrical approach alone yields valuable insight into the mixing of granular materials, there are a number of effects which this technique fails to capture. Precession is but one of the material-dependent mechanisms which cannot be incorporated in a purely geometrical description of granular mixing. Similarly, particle segregation is not captured with this method either. However, by combining particle dynamics techniques with the geometrical approach —in essence, by *focusing* the particle dynamics simulation only where it is needed—a new hybrid method of mixer simulation, which is both more accurate than the geometrical method and much faster than the particle dynamics method, can be achieved. This novel numerical technique can easily and quickly examine a wide range of particle properties, so that the relative importance of each can be easily assessed. In doing so, it may be possible to propose a criterion which will aid in determining *a priori* which combinations of material will be successfully mixed in tumbling containers.

Acknowledgment

This work was supported by the Dept. of Energy, Division of Basic Energy Sciences and by ALCOA. We wish to thank the support of Dr. Phil Hseih.

Notation

a = particle radius, m
$f_{n,e}$ = elastic normal force, kg·m/s^2
k_d = damping coefficient, kg/m·s
L = characteristic length of a horizontal drum (half-length of the axis of rotation), m
δ = boundary layer width, m
θ_p = precession angle, degrees (degrees per time)
μ = coefficient of friction

Literature Cited

Baxter, G. W., and R. Behringer, "Cellular Automata Models for the Flow of Granular Materials," *Phys. D*, **51**, 465 (1991).
Behringer, R. P., "The Dynamics of Flowing Sand," *Nonlin. Sci. Today*, **3**, 1 (1993).
Bridgwater, J., W. S. Foo, and D. J. Stephens, "Particle Mixing and Segregation in Failure Zones," *Pow. Tech.*, **41**, 147 (1985).
Bridgwater, J., "Fundamental Powder Mixing Mechanisms," *Pow. Tech.*, **15**, 215 (1976).
Bridgwater, J., D. F. Bagster, S. F. Chen, and J. H. Hallam, "Geometric and Dynamic Similarity in Particle Mixing," *Pow. Tech.*, **2**, 198 (1968).
Broadbelt, C. J., J. Bridgwater, D. J. Parker, S. T. Keningley, and P. Knight, "Phenomenological Study of a Batch Mixer Using a Positron Camera," *Pow. Tech.*, **76**, 317 (1993).
Buchholtz, V., and T. Poschel, "Numerical Investigations of the Evolution of Sandpiles," *Physica A*, **202**, 390 (1994).
Bui, R. T., J. Perron, and M. Read, "Model-Based Optimization of the Operation of the Coke Calcining Kiln," *Carbon*, **31**, 1139 (1993).
Campbell, C. S., "Rapid Granular Flows," *Ann. Revs. Fluid Mech.*, **22**, 57 (1989).
Campbell, C. S., and C. E. Brennen, "Chute Flows of Granular Material: Some Computer Simulations," *J. Appl. Mech.*, **52**, 172 (1985).
Carley-Macauly, K. W., and M. B. Donald, "The Mixing of Solids in Tumbling Mixers: I," *Chem. Eng. Sci.*, **17**, 493 (1962).
Carley-Macauly, K. W., and M. B. Donald, "The Mixing of Solids in Tumbling Mixers: II," *Chem. Eng. Sci.*, **19**, 191 (1964).
Cundall, P. A., and O. D. L. Strack, "A Discrete Numerical Model for Granular Assemblies," *Geotechnique*, **29**, 47 (1979).
Fan, L. T., Y. Chen, and F. S. Lai, "Recent Developments in Solids Mixing," *Pow. Tech.*, **61**, 255 (1990).
Franjione, J. G., C. W. Leong, and J. M. Ottino, "Symmetries within Chaos: A Route to Effective Mixing," *Phys. Fluids A*, **1**, 1772 (1989).
Hertz, H., "Ueber die Berhrungfester Elastischer Korper," *J. Renie Angew. Math*, **92**, 156 (1881).
Hersey, J. A., "Powder Mixing: Theory and Practice in Pharmacy," *Pow. Tech.*, **15**, 149 (1976).
Hirosue, H., "Axial Mixing of Particles in Rotary Dryers and Coolers," *J. Chem. Eng. Jap.*, **13**, 365 (1980).
Hogg, R., D. S. Cahn, T. W. Healy, and D. W. Fuerstenau, "Diffusional Mixing in an Ideal System," *Nature*, **209**, 494 (1966a).
Hogg, R., D. S. Cahn, T. W. Healy, and D. W. Fuerstenau, "Diffusional Mixing in an Ideal System," *Chem. Eng. Sci.*, **21**, 1025 (1966b).
Hwang, C. L., and R. Hogg, "Diffusive Mixing in Flowing Powders," *Pow. Tech.*, **26**, 83 (1980).
Jaeger, H. M., and S. R. Nagel, "Physics of the Granular State," *Science*, **255**, 1523 (1992).
Kaye, B. H., and D. B. Sparrow, "Role of Surface Diffusion as a Mixing Mechanism in a Barrel-Mixer," *Ind. Chem.*, **40**, 200 (1964).
Khakhar, D. V., J. J. McCarthy, T. Shinbrot, and J. M. Ottino, "Transverse Flow and Mixing of Granular Materials in a Rotating Cylinder," *Phys. of Fluids*, in press (1997).
Lacey, P. M., "Developments in the Theory of Particle Mixing," *J. Appl. Chem.*, **4**, 257 (1954).
Lee, J., and H. J. Herrmann, "Angle of Repose and Angle of Marginal Stability: Molecular Dynamics of Granular Particles," *J. Phys. A: Math. Gen.*, **26**, 373 (1993).
Lee, J., "Avalanches in (1+1)-Dimensional Piles: A Molecular Dynamics Study," *J. Phys. I France*, **3**, 2017 (1993).
Liu, C. H., S. R. Nagel, D. A. Schecter, S. N. Coppersmith, S. Majumdar, O. Narayan, and T. A. Witten, "Force Fluctuations in Bead Packs," *Sci.*, **269**, 513 (1995).
Mehta, A., ed., *Granular Matter: An Interdisciplinary Approach*, Springer-Verlag, New York (1994).
Mehta, A., and S. F. Edwards, "Statistical Mechanics of Powder Mixtures," *Phys. A*, **157**, 1091 (1989).
Metcalfe, G., T. Shinbrot, J. J. McCarthy, and J. M. Ottino, "Avalanche Mixing of Granular Solids," *Nature*, **374**, 39 (1995).
Mindlin, R. D., "Compliance of Elastic Bodies in Contact," *J. Appl. Mech.*, **16**, 256 (1949).
Mohanty, K. K., J. M. Ottino, and H. T. Davis, "Reaction and Transport in Disordered Composite Media: Introduction of Percolation Concepts," *Chem. Eng. Sci.*, **37**, 905 (1982).
Nakagawa, M., S. A. Altobelli, A. Caprihan, E. Fukushima, and E. K. Jeong, "Non-Invasive Measurements of Granular Flows by Magnetic Resonance Imaging," *Expr. Fluids*, **16**, 54 (1993).
Nikitidis, M. S., M. E. Hosseini-Ashrafi, U. Tuzun, and N. M. Spyrou, "Tomographic Measurements of Granular Flows in Gases and Liquids," *KONA*, **12**, 53 (1994).
Ottino, J. M., F. J. Muzzio, M. Tjahjadi, J. G. Franjione, S. C. Jana, and H. A. Kusch, "Chaos, Symmetry, and Self-Similarity: Exploiting Order and Disorder in Mixing Processes," *Sci.*, **257**, 754 (1992).
Ottino, J. M., *The Kinematics of Mixing: Stretching, Chaos, and Transport*, Cambridge University Press, Cambridge (1990).

Peralt, B. A., and J. A. Yorke, "Continuous Avalanche Mixing of Granular Solids in a Rotating Drum," *Europhys. Lett.*, submitted (1995).
Perron, J., R. T. Bui, and H. T. Nguyen, "Modélisation d'un Four de Calcinacion du Coke de Pétrole: I. Le Modèle," *Canad. J. Chem. Eng.*, **70**, 1108 (1992).
Perron, J., and R. T. Bui, "Rotary Cylinders: Solid Transport Prediction by Dimensional and Rheological Analysis," *Can. J. Chem. Eng.*, **68**, 61 (1990).
Poux, M., P. Fayolle, J. Bertrand, D. Bridoux, and J. Bousquet, "Powder Mixing," *Pow. Tech.*, **68**, 213 (1991).
Rutgers, R., "Longitudinal Mixing of Granular Material Flowing through a Rotating Cylinder," *Chem. Eng. Sci.*, **20**, 1079 (1965).
Tsuji, Y., "Discrete Particle Simulation of Gas-Solid Flows (from Dilute to Dense Flows)," *KONA*, **11**, 57 (1993).
Tsuji, Y., T. Tanaka, and T. Ishida, "Lagrangian Numerical Simulation of Plug Flow of Cohesionless Particles in a Horizontal Pipe," *Powder Technol.*, **71**, 239 (1992).
Walton, O. R., "Numerical Simulation of Inclined Chute Flows of Monodisperse, Inelastic, Frictional Spheres," *Mech. Mat.*, **16**, 239 (1993).
Walton, O. R., and R. L. Braun, "Simulation of Rotary-Drum and Repose Tests for Frictional Spheres and Rigid Spheres Clusters," *Joint DOE/NSF Workshop on Flow of Particulates and Fluids*, Ithaca, NY, p. 1 (Sept. 29–Oct. 1, 1993).
Walton, O. R., "Application of Molecular Dynamics to Macroscopic Particles," *Int. J. Eng. Sci.*, **22**, 1097 (1984).
Wang, R. H., and L. T. Fan, "Methods for Scaling up Tumbling Mixers," *Chem. Eng.*, 88 (May 27, 1974).
Weidenbaum, S. S., "Mixing of Solids," *Advances in Chemical Engineering*, Vol. 2, T. B. Drew and J. W. Hoopes, eds., Academic Press, New York, p. 211 (1958).
Weitz, D. A., *MRS Bulletin*, **XIX**, 5, articles pp. 11 and 25 (1994).
Wightman, C., P. R. Mort, F. J. Muzzio, R. E. Riman, and R. K. Gleason, "The Structure of Mixtures of Particles Generated by Time-Dependent Flows," *Powder Technol.*, **84**, 231 (1995).
Wolf, E., "Geometrical Aspects of Granular Solids Mixing," MS Thesis, Northwestern Univ., Evanston, IL (1995).
Zablotny, W. W., "The Movement of the Charge in Rotary Kilns," *Int. Chem. Eng.*, **5**, 360 (1965).

Manuscript received Feb. 5, 1996, and revision received June 27, 1996.